Available online at www.sciencedirect.com
SCIENCE DIRECT®
Journal of Physics and Chemistry of Solids 65 (2004) 1759–1764
JOURNAL OF PHYSICS AND CHEMISTRY OF SOLIDS
www.elsevier.com/locate/jpcs

Synthesis and characterization of a new monophosphate $[2,5\text{-}(CH_3)_2C_6H_3NH_3]H_2PO_4$

K. Kaabi, C. Ben Nasr, M. Rzaigui*

Laboratoire de Chimie des Matériaux, Faculté des Sciences de Bizerte, 7021 Zarzouna, Bizerte, Tunisia

Received 25 November 2003; revised 20 February 2004; accepted 12 April 2004

Abstract

Chemical preparation, calorimetric studies, crystal structure and spectroscopic investigations are given for a new noncentrosymmetric organic cation monophosphate $[2,5\text{-}(CH_3)_2C_6H_3NH_3]H_2PO_4$. This compound is orthorhombic $P2_12_12_1$ with the following unit-cell parameters: $a = 5.872(4)$, $b = 20.984(3)$, $c = 8.465(1)$ Å, $Z = 4$, $V = 1043.0(5)$ Å^3 and $D_x = 1.396$ g cm^{-3}. Crystal structure has been solved and refined to $R = 0.048$ using 2526 independent reflections. Structure can be described as an inorganic layer parallel to (a, b) planes between which organic groups $[2,5\text{-}(CH_3)_2C_6H_3NH_3]^+$ are located. Multiple hydrogen bonds connecting the different entities of compound thrust upon three-dimensional network a noncentrosymmetric configuration.

Keywords: A. Optical materials; B. Chemical synthesis; C. X-ray diffraction; C. Infrared spectroscopy; C. Thermogravimetric analysis (TGA); D. Crystal structure

1. Introduction

Crystal engineering of non-linear optical crystals [1] is supported by some observations: (i) the anchorage of organic cations onto inorganic subnetworks through multiple and short hydrogen bonds providing the packing with the cohesion observed in the ionic inorganic crystals; (ii) a blue shift of the crystal transparency resulting from the less polarizable nature of the protonated 2,5-dimethylphenylaminium cation as compared to an equivalent purely organic crystal; (iii) the building of acentric framework without using polarisable chiral entities. In this context, we report the synthesis and the crystal structure of a new organic cation monophosphate: $[2,5\text{-}(CH_3)_2C_6H_3NH_3]H_2PO_4$. This compound was synthesized within a systematic search on new materials resulting from the association of organic and inorganic entities, which could be of particular interest in non-linear optics.

2. Experimental

2.1. Chemical preparation

Crystals of the title compound $[2,5\text{-}(CH_3)_2C_6H_3NH_3]\text{-}H_2PO_4$ were prepared by slowly adding, at room temperature, 6.8 cm^3 of H_3PO_4 (85%, $d = 1.7$) to an alcoholic solution containing 12.6 cm^3 of 2,5-dimethylaniline (98%, $d = 0.98$). A crystalline precipitate was formed resulting from the following reaction:

$$2,5\text{-}(CH_3)_2C_6H_3NH_2 + H_3PO_4 \rightarrow [2,5\text{-}(CH_3)_2C_6H_3NH_3]H_2PO_4$$

After dissolution by adding H_2O the solution is slowly evaporated at room temperature during several days until the formation of transparent prismatic crystals with suitable dimensions for crystallographic study. The crystals are stable for months in normal conditions of temperature and humidity.

2.2. Investigation techniques

The title compound has been studied by various physico-chemical methods.

* Corresponding author. Tel.: +216-72-591-906; fax: +216-72-590-566.
E-mail address: mohamed.rzaigui@fsb.rnu.tn (M. Rzaigui).

0022-3697/$ - see front matter © 2004 Elsevier Ltd. All rights reserved.
doi:10.1016/j.jpcs.2004.04.003

2.2.1. X-ray diffraction

The intensity data collection was performed using a MACH3 Enraf–Nonius diffractometer. The experimental conditions of data collection, the strategy followed for the structure determination and its final results are given in Table 1.

2.2.2. Thermal behavior

Thermal analysis was performed using the 'multimodule 92 Setaram' analyzer operating from room temperature up to 450 °C at an average heating rate of 5 °C/min.

2.2.3. Infrared spectroscopy

Spectra were recorded in the range 4000–200 cm^{-1} with a 'Perkin-Elmer FTIR' spectrophotometer 1000 using samples dispersed in spectroscopically pure KBr pellets.

Table 1
Crystal data, experimental parameters used for the intensity collection, strategy and final results of the structure determination

I-Crystal data	
Formula: $[2,5\text{-}(CH_3)_2C_6H_3NH_3]H_2PO_4$	$F_w = 219.18$
System: orthorhombic	Space group: $P2_12_12_1$
$a = 5.872(4)$, $b = 20.984(3)$, $c = 8.465(1)$ Å	$V = 1143.0(1)$ Å^3, $Z = 4$
Refinement of unit cell parameters with 25 reflections ($10° < \theta < 12°$)	
$\rho_{cal.} = 1.396$ g. cm^{-3}	$F(000) = 464$
Morphology: prism	Crystal size (mm): $0.40 \times 0.35 \times 0.30$
Linear absorption factor: μ (Mo Kα) = 2.525 cm^{-1}	
II-Intensity measurements	
Diffractometer: Enraf–Nonius MACH3 (296 K)	Wavelength: Ag K$\bar{\alpha}$ (0.5608 Å)
Scan mode: $\omega 2\theta$	Theta range: 2–30°
Measurement area: h, k, l	$h_{max.} = 10$, $k_{max.} = 37$, $l_{max.} = 15$
Nb. of scanned reflections: 3528	Nb. of independent reflections: 3528
Two intensity and orientation control reflections: 0 7 4 and 0 $\bar{7}$ 4, no variation, every 400	
III-Structure determination	
Lorentz and polarization corrections	Absorption correction: empirical ($T_{max} = 1.000$, $T_{min} = 0.738$)
Determination: a direct method SIR92 [2]	Program used: teXsan [3]
Thermal displacement parameters: isotropic for H atoms, anisotropic for non-H atoms	
H atoms position were located by Fourier difference syntheses	
Unique reflections included: 2694 with $I > 2\sigma(I)$	Weighting scheme: sigma
Agreement factors R : 0.038, R_w : 0.055	Refined parameters: 183
Residual Fourier density: $-0.25 < \rho < 0.25$ e Å^{-3}	Largest shift/error: 0.8
Drawings made with Diamond [4]	Esd: 1.00

2.2.4. NMR spectroscopy

All NMR spectra were recorded on a bruker DSX-300 spectrometer operating at 75.49 MHz for ^{13}C and 121.51 MHz for ^{31}P with a classical 4 mm probehead allowing spinning rates up to 10 kHz. ^{13}C NMR chemical shifts are given relative to tetramethylsiline and ^{31}P ones relative to 85% H_3PO_4 (external references, precision 0.5 ppm). Phosphorous spectra were recorded under classical MAS conditions while the carbon ones were recorded by use of cross-polarization from protons (contact time 5 ms). Analysis of MAS-NMR spectrum was carried out by using the Bruker program WINTFIT [5]. To assign NMR components to the various carbons of the organic groups, ab initio calculations were performed with the GAUSSIAN 98 software [6].

3. Results and discussion

3.1. Structure description

Structural determination shows that the title compound crystallizes in the orthorhombic system with the noncentrosymmetric space group, $P2_12_12_1$, which is confirmed by a positive second harmonic generation powder test observed on a sample illuminated by YAG Nd^{3+} laser radiation at 1.06 μm.

The final atomic coordinates of all non-hydrogen atoms of $[2,5\text{-}(CH_3)_2C_6H_3NH_3]H_2PO_4$ and their Beq are given in Table 2. Those of hydrogen atoms, determined by difference Fourier maps and not refined, are not given in order to shorten the table. The main geometrical features of different entities are reported in Table 3.

A perspective view of the asymmetric unit of the structure is depicted in Fig. 1, while the complete atomic arrangement is shown in Fig. 2. This latter shows that the $H_2PO_4^-$ inorganic entities have a layered organization around the planes $y = 1/4$ and 3/4.

Table 2
Final atomic coordinates and Beq for the non-hydrogen atoms

Atoms	$x(\sigma)$	$y(\sigma)$	$z(\sigma)$	Beq (Å^2)
P	1.38335(5)	0.22775(1)	1.33199(4)	1.973(4)
O(1)	1.2354(2)	0.17284(5)	1.4021(2)	3.01(2)
O(2)	1.6284(2)	0.19800(5)	1.31809(13)	2.89(2)
O(3)	1.3883(2)	0.28370(4)	1.44338(13)	2.53(2)
O(4)	1.3038(2)	0.24202(5)	1.16788(13)	3.04(2)
N	0.9415(2)	0.17362(5)	1.0537(1)	2.23(2)
C(1)	0.9893(2)	0.10787(6)	1.0089(2)	2.25(2)
C(2)	1.1786(3)	0.09513(7)	0.9152(2)	2.78(2)
C(3)	1.2176(3)	0.03097(8)	0.8787(3)	3.69(3)
C(4)	1.0719(4)	0.01672(7)	0.9303(3)	3.88(3)
C(5)	0.8806(4)	−0.00300(7)	1.0194(2)	3.31(3)
C(6)	0.8424(3)	0.06069(7)	1.0606(2)	2.72(2)
C(7)	1.3319(4)	0.14601(10)	0.8514(3)	3.90(3)
C(8)	0.7194(5)	0.05418(9)	1.0702(4)	4.88(5)

Note. Esd are given in parentheses.

Table 3
Main interatomic distances (Å) and angles (°) in $[2,5\text{-}(CH_3)_2C_6H_3NH_3]H_2PO_4$ atomic arrangement

The PO_4 tetrahedron				
P	O(1)	O(2)	O(3)	O(4)
O(1)	*1.560(1)*	2.471(2)	2.518(2)	2.490(2)
O(2)	104.15(8)	*1.573(2)*	2.519(2)	2.471(3)
O(3)	110.39(7)	109.78(7)	*1.506(1)*	2.540(2)
O(4)	109.02(8)	107.21(9)	115.56 (1)	*1.496(1)*
O(1)–H(1)	0.81(2)	O(2)–H(2)	0.79(3)	
P–O(1)–H(1)	115(2)	P–O(2)–H(2)	117(2)	
$[2,5\text{-}(CH_3)_2C_6H_3NH_3]^+$ group				
C(1)–C(2)	1.391(2)	C(1)–C(2)–C(3)	116.2(2)	
C(2)–C(3)	1.400(2)	C(1)–C(2)–C(7)	123.3(1)	
C(2)–C(7)	1.498(3)	C(3)–C(2)–C(7)	120.5(2)	
C(3)–C(4)	1.387(3)	C(2)–C(3)–C(4)	121.6(2)	
C(4)–C(5)	1.384(3)	C(3)–C(4)–C(5)	121.5(2)	
C(5)–C(6)	1.399(2)	C(4)–C(5)–C(6)	117.7(2)	
C(5)–C(8)	1.494(3)	C(4)–C(5)–C(8)	121.4(2)	
C(6)–C(1)	1.384(2)	C(6)–C(5)–C(8)	120.9(2)	
N–C(1)	1.458(2)	C(5)–C(6)–C(1)	120.3(2)	
N–H(3)	0.98(3)	C(6)–C(1)–C(2)	122.7(1)	
N–H(4)	0.95(3)	N–C(1)–C(2)	118.9(1)	
N–H(5)	0.95(3)	N–C(1)–C(6)	118.3(1)	
		C(1)–N–H(3)	113(5)	
		C(1)–N–H(4)	115(1)	
		C(1)–N–H(5)	110(1)	
The hydrogen bonds				
O(N)–H···O	O(N)–H	H···O	O(N)···O	O(N)–H···O
O(1)–H(1)···O(3)	0.81(2)	1.78(2)	2.588(2)	174(2)
O(2)–H(2)···O(3)	0.79(3)	1.78(3)	2.560(2)	167(2)
N–H(3)···O(4)	0.98(3)	1.73(2)	2.703(2)	170(2)
N–H(4)···O(2)	0.95(3)	2.00(3)	2.941(2)	173(2)
N–H(5).···O(4)	0.95(3)	1.80(3)	2.742(2)	170(2)

Note. Esd are given in parentheses.

Fig. 3 represents a projection of such a layer located in the plane $y = 3/4$. It shows that the $H_2PO_4^-$ groups are connected by strong hydrogen bonds to form infinite corrugated chains in the *c*-direction of composition $(H_2PO_4)_n^{n-}$. These chains are themselves interconnected by means of N–H···O hydrogen bonds originating from the NH_3^+ group, so as to build inorganic layers formed by $H_2PO_4^-$ and NH_3^+ groups. The P–P distance between H_2PO_4 tetrahedra: 4.194(3) is slightly shorter than that observed in $NH_3(CH_2)_4NH_3HPO_4{\cdot}H_2O$ [7]. This is probably due to the presence of two acidic hydrogen atoms on the PO_4, which is favorable for the formation of strong hydrogen bonds. The detailed geometry of $H_2PO_4^-$ groups shows that the P–O bonds are significantly shorter (1.469(1), 1.506(1) Å) than the P–OH bonds (1.560(1), 1.573(1) Å). This is in agreement with the data relative to the protonated oxoanions [8]. Relatively short distances, from 1.73(2) to 2.00(3) Å, characterize all H···O bonds, which maintain the cohesion of this arrangement. It is worth noting that the O···O distances involved in the hydrogen bonds (2.560(2)–2.588(2) Å) are of the same order of magnitude as the O–O in the PO_4 tetrahedron (2.471(2)–2.540(2) Å), this should allow us to consider the $[H_2PO_4]_n^{n-}$ subnetwork as a polyanion.

The 2,5-dimethylphenylammonium $[2,5\text{-}(CH_3)_2C_6H_3\text{-}NH_3]^+$ groups are anchored onto successive inorganic layers through hydrogen bonds involving the hydrogen atoms of the NH_3 groups with H(N)···O distances varying between 1.73(2) and 2.00(3) Å. N–C and C–C distances and C–C–N and C–C–C angles in this group are reported in Table 3.

The $2,5\text{-}(CH_3)_2C_6H_3NH_2$ organic molecule, containing delocated and asymmetric Π-bonds, is highly polarizable entity in which transparency could be controlled. This property favours the formation of noncentrosymmetric materials as found with benzylamine $C_6H_5CH_2NH_2$ and paraphenolamine $1,4\text{-}HOC_6H_4NH_2$ which reacts with H_3PO_4 to form $(C_6H_5CH_2NH_2)H_2PO_4$ [9] and $(1,4\text{-}HOC_6\text{-}H_4NH_2)H_2PO_4$ [10] salts for Second Harmonic Generation.

3.2. Thermal analysis

The two curves corresponding to DTA and TGA analysis in argon are given in Fig. 4. The DTA curve shows a series of weak peaks in a wide temperature range (190–475 °C), the most important one appears at about 203 °C. The TGA curve shows a continuous weight loss in all this temperature area. So, the corresponding phenomena could be interpreted by $H_2PO_4^-$ condensation and a $[2,5\text{-}(CH_3)_2C_6H_3NH_3]^+$

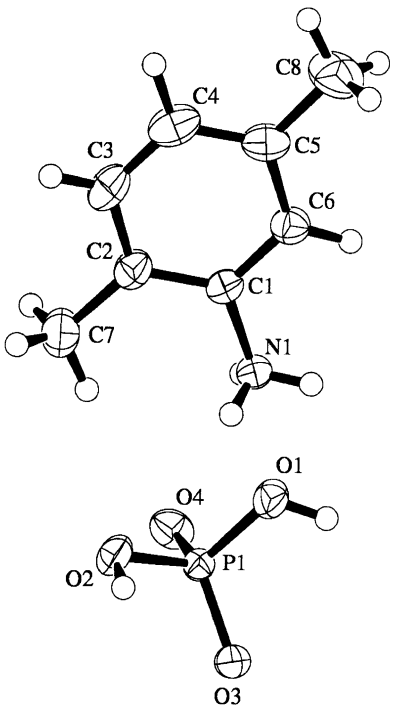

Fig. 1. Asymmetric unit of $[2,5\text{-}(CH_3)_2C_6H_3NH_3]H_2PO_4$. Thermal ellipsoids are shown at 40% probability.

degradation leading to viscous matter of polyphosphoric acids with a carbon black residue.

3.3. Infrared spectroscopy

The monophosphate vibrations have been investigated obviously [11,12]. The theoretical group analysis applied to

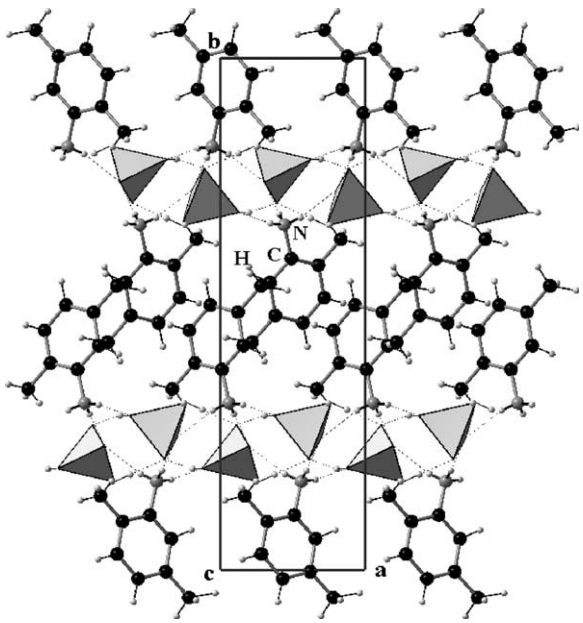

Fig. 2. Arrangement of $[2,5\text{-}(CH_3O)_2C_6H_3NH_3]H_2PO_4$ in projection along the c-axis. PO_4 is given in the tetrahedral representation. Hydrogen bonds are denoted by dotted lines.

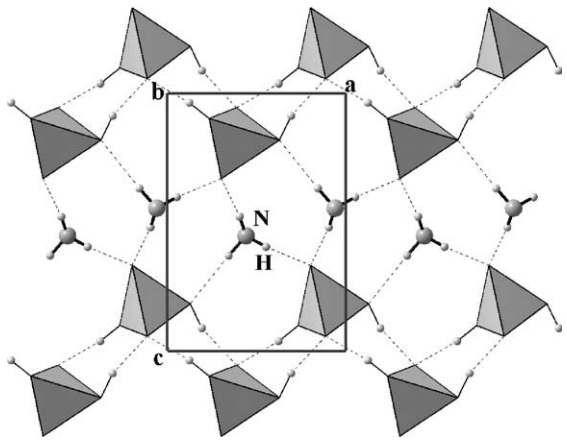

Fig. 3. Projection along the b-axis of the inorganic layer in $[2,5(CH_3)_2\text{-}C_6H_3NH_3]H_2PO_4$ structure. Note: organic radical are omitted for the clarity of the figure.

an isolated PO_4 in its ideal T_d local symmetry to the nine normal modes fundamentals of vibrations. The normal modes are given by the representation:

$$\Gamma_{\text{int}} = A_1 + E_2 + 2F_2$$

Four are stretching modes, one is symmetric $\nu_s(A_1)$ and three are asymmetric $\nu_{as}(F_2)$:

$$\Gamma_{\text{str}} = A_1 + F_2$$

Five are bending modes, two are symmetric $\delta_s(E_2)$ and three are asymmetric $\delta_s(F_2)$:

$$\Gamma_{\text{ben}} = E_2 + F_2$$

Among these, only the F_2 is active in IR and E_2, A_1 and F_2 are active in Raman. Nevertheless, crystals of the latter compound belong to the $P2_12_12_1$ space group and there are four units PO_4 per cell, at a site of C_1 symmetry. According to the literature and to the theoretical group analysis of the crystal of the title compound, there are 36 normal modes classified in this point group:

$$\Gamma_{\text{int}} = 9A + 9B_1 + 9B_2 + 9B_3$$

In Table 4 are attributed the remaining observed bands in the spectrum in Fig. 5 to the stretching and bending modes corresponding to the different organic and inorganic groups.

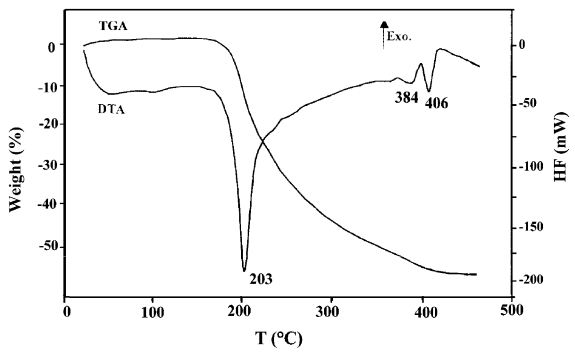

Fig. 4. DTA and TGA curves of $[2,5\text{-}(CH_3)_2C_6H_3NH_3]H_2PO_4$ at rising temperature.

Table 4
IR frequencies and assignments in the stretching and bending domain of PO_4^{3-} in $[2,5\text{-}(CH_3O)_2C_6H_3NH_3]H_2PO_4$

	Free ion PO_4^{3-} T_d	site group C_1	factor group D_2			Obs. IR frequencies (cm^{-1})
Motions	Modes	Modes	Modes	Ra	IR	
ν_{as}	F_2	3A	3A	+	–	1160 vw
			$3B_1$	+	+	1117 vw
			$3B_2$	+	+	1047 vw
			$3B_3$	+	+	
ν_s + ($\delta(C_{aryl}\text{-}H)_{ip}$ + ν(C-C))	A	A	A	+	–	901 m
			B_1	+	+	856 vw
			B_2	+	+	848 w
			B_3	+	+	827 w
						803 s
δ_{as} + $\delta(C_{aryl}\text{-}H)_{op}$	F_2	3A	3A	+	–	577 w
			$3B_1$	+	+	558 vw
			$3B_2$	+	+	533 w
			$3B_3$	+	+	524 vs
δ_s + δ(C=C)	E_2	2A	2A	+	–	485 w
			$2B_1$	+	+	447 s
			$2B_2$	+	+	413 vw
			$2B_3$	+	+	396 m

Note: vs, very strong; s, strong; m, middle; w, weak; vw, very weak.

Frequencies in the range 4000–1400 cm^{-1} are attributed to C(N)–H stretching and bending modes [13]. Absorption bands in the range 1400–1200 cm^{-1}, corresponding to stretching vibrations of C–N bonds and O–H groups [14]. The two stretching vibration bands characteristics of a PO_4 tetrahedron ν_s and ν_{as} are observed about 1200–1000 and 1000–850 cm^{-1}, those ranging from 650–500 to 500–300 cm^{-1} attributed to bending modes δ_s and δ_{as} of PO_4 [11,12]. We note that the supplementary frequencies in the $\nu_s(PO_4)$ domain are attributed to the bending modes $\delta(C_{aryl} - H)_{ip}$ [15].

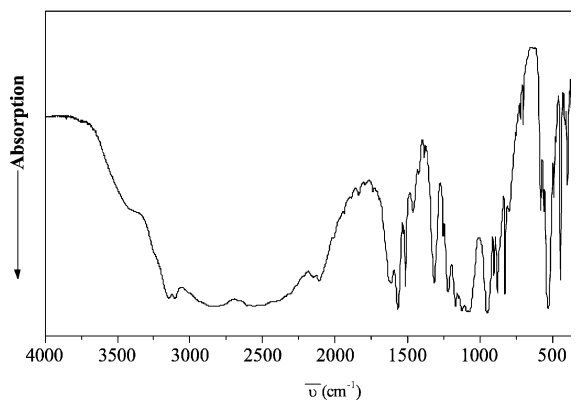

Fig. 5. IR-spectra of $[2,5\text{-}(CH_3)_2C_6H_3NH_3]H_2PO_4$.

However, the experimental and theoretical results are not compatible, this can be explained by the interactions between the different PO_4^{3-} ions, because the unit cell of this compound contains four anions.

3.4. NMR spectroscopy

Proton decoupled ^{31}P MAS-NMR spectrum of crystalline monophosphate $[2,5\text{-}(CH_3)_2C_6H_3NH_3]H_2PO_4$ is given in Fig. 6. It exhibits only one peak with two corresponding satellite spinning side bands spaced at equal intervals (spinning rate of the sample expressed in ppm). The corresponding chemical shift value −0.02 ppm was

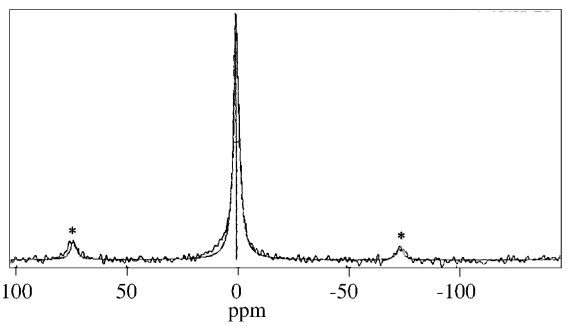

Fig. 6. Theoretical and experimental ^{31}P MAS-NMR spectrum of crystalline dihydrogenomonophosphate $[2,5\text{-}(CH_3)_2C_6H_3NH_3]H_2PO_4$. * Spinning side bands.

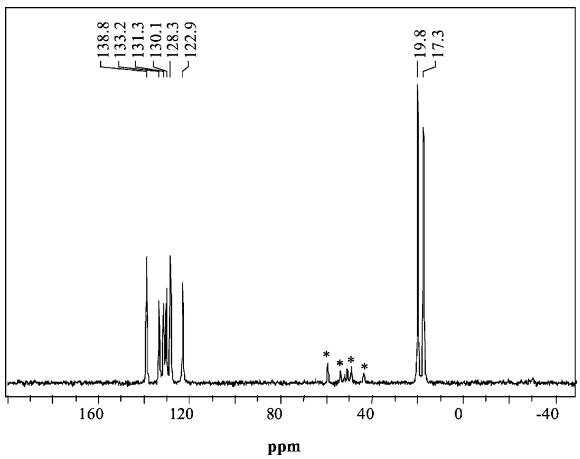

Fig. 7. ^{13}C CP-MAS-NMR spectrum of crystalline dihydrogenomonophosphate $[2,5\text{-}(CH_3)_2C_6H_3NH_3]H_2PO_4$. * Spinning side bands.

recorded with respect to 85% H_3PO_4 (negative chemical shifts are towards higher fields in spectrum). This chemical shift value agrees with those of monophosphates (between -10 and $+5$ ppm), depending on the compound [16–18]. The existence of a single peak in the region analyzed indicates the presence of only one crystallographic site in the unit cell of this monophosphate, which agrees with the X-ray results.

On the other hand, distortions of the polyhedra are responsible for observed chemical shift anisotropies and for detection of spinning side band patterns covering important region of ^{31}P NMR spectra. Spectral region occupied by these bands are proportional to tetrahedral distortions. From this fact, NMR patterns could be used to monitor distortion. In order to analyze this point, the experimental envelope was deconvoluted, determining for the single NMR component σ_{iso}, $\Delta\sigma$ and η. The obtained results were $\sigma_{iso} = -0.02$ ppm, $\Delta\sigma = -44.95$ ppm and $\eta = 0.00$. This asymmetric parameter equal to zero suggests the existence of an axial distortion of PO_4 tetrahedra.

The ^{13}C CP-MAS NMR spectrum of the title compound is given in Fig. 7. The carbon atoms of the organic group are labeled as depicted below

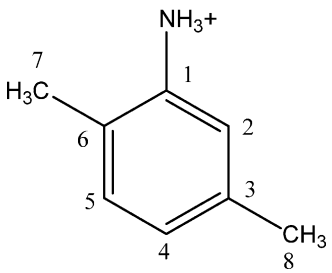

To assign NMR components to different carbon atoms we used ab initio calculations. The chemical shifts of the eight carbon atoms were calculated and the results are regrouped in Table 5.

Table 5
Calculated (δ_{iso}) and experimental (δ_{exp}) chemical shifts of the organic groups carbon atoms

Carbon atoms	C1	C2	C3	C4	C5	C6	C7	C8
δ_{iso} (ppm)	60.6	57.1	31.5	39.7	42.4	52.0	166.3	159.1
δ_{exp} (ppm)	122.9	128.3	138.3	133.2	131.3	130.1	17.4	19.8

δ_{iso} being the absolute chemical shift and the relative chemical shifts, such as those measured experimentally, correspond to the difference

$$\delta_{exp} = \delta_{ref} - \delta_{iso}$$

thus, we can propose the attribution gathered in Table 5.

Acknowledgements

We would like to thank the Secretary of State for Scientific Research and Technology for their support, in this work.

References

[1] R. Masse, M. Bagieu-Beucher, J. Pecault, J.P. Levy, J. Zyss, Nonlin. Opt. 5 (1993) 413–423.
[2] A. Altomare, M. Cascarano, C. Giacovazzo, A. Guagliardi, Completation and refinement of crystal structures with Sir 92, J. Appl. Cryst. 26 (1993) 343–350.
[3] teXsan for Windows Version 1.03, Molecular Structure Corporation, Single Crystal Structure Analysis Software, Version 1.03, MSC, 3200 Research Forest Drive, The Woodlands, TX 77381, USA, 1997.
[4] K. Brandenburg, Diamond Version 2.0 (1998).
[5] Bruker WINTFIT Program, Bruker Rep. 40 (1994) 431–435.
[6] M.J. Frisch, et al., GAUSSIAN 98, A.7, Gaussian Inc., Pittsburgh, PA, 1998.
[7] S. Kamoun, A. Jouini, J. Solid State Chem. 89 (1990) 67–74.
[8] J. Herzfeld, A.L. Berger, J. Chem. Phys. 73 (1980) 6021–6030.
[9] C.B. Aakeroy, P.B. Hitchcock, B.D. Moyle, K.R. Seddon, J. Chem. Soc. Commun. (1989) 1856–1859.
[10] E.H. Soumhi, A. Driss et, T. Jouini, Mater. Res. Bull. 29 (1994) 767–773.
[11] G. Herzberg, Infrared and Raman Spectra of Polyatomic Molecules, Van Nostraand, New York, 1975.
[12] K. Nakamoto, Infrared and Raman Spectra of Inoganic and Coordination Compounds, Wiley/Intersciences, New York, 1984.
[13] M. Charfi, A. Jouini, J. Solid State Chem. 127 (1996) 9–18.
[14] B. Stuart, Modern Infrared Spectroscopy, Wiley, England, 1996.
[15] R.M. Silverstein, G.C. Bassler, T.C. Morill, Spectrometric Identification of Organic Compounds, 3rd ed., Wiley, New York, 1974.
[16] A.R. Grimmer, U. Haubenreisser, Chem. Phys. Lett. 99 (1983) 487–490.
[17] D. Mûller, E. Jahn, G. Ladwig, U. Haubenreisser, Chem. Phys. Lett. 109 (1984) 332–336.
[18] S. Prabhakar, K.J. Rao, C.N.R. Rao, Chem. Phys. Lett. 139 (1987) 96–102.